Preparation and Characterization of Monodisperse PbSe Semiconductor Nanocrystals in a Noncoordinating Solvent

William W. Yu, Joshua C. Falkner, Bertram S. Shih, and Vicki L. Colvin*

Department of Chemistry, Rice University, 6100 Main Street, Houston, Texas 77005

Received March 27, 2004. Revised Manuscript Received June 2, 2004

Spherical PbSe semiconductor nanocrystals with near-infrared absorption of 1100−2520 nm (corresponding to diameters of 3−13 nm) were synthesized in a noncoordinating solvent (1-octadecene). The as-prepared PbSe semiconductor nanocrystals have very narrow size distributions ($\sigma \cong 5-7\%$) without any postsynthetic size selection. High-resolution transmission electron microscopy (TEM), electron diffraction, and X-ray diffraction show that the nanocrystalline particles are single domains of rock-salt PbSe. A water-soluble form of these materials was generated through simple surface treatments.

Introduction

Semiconductor nanocrystals have attracted great attention for their unique size-dependent behavior; their optical properties in particular differ greatly from the corresponding molecular and bulk materials.[1−3] Quantum confinement in nanocrystals leads to tunable blue shifts in both optical absorption and emission spectra with decreasing nanocrystal size. This phenomena has been extensively studied in monodisperse and size-controlled II−VI semiconductor nanocrystals (CdS, CdSe, and CdTe).[4−6] Many applications which rely on the size tunability and high quantum yields of these systems have also been proposed and, in some cases, developed into commercial products.[7−17]

Comparatively less is known about the related family of nanoscale lead chalocogenides. As direct gap semiconductors in the bulk phase, they should exhibit similar size-dependent behavior to the cadmium systems; however, the very large Bohr radii in lead materials (20−46 nm), as compared to cadmium systems (4−10 nm), permits their optical properties to be evaluated in the limit of extremely strong quantum confinement.[18] In this regime, theoretical predictions of both maximum absorbance as well as oscillator strength are at odds with experimentally measured values.[19] Additionally, lead chalcogenide nanocrystals emit near-infrared (NIR) light, and their high nonlinearities make them excellent materials for optical switches.[18] The near-infrared emission is also an ideal property for biological imaging; tissue has a window in absorbance between 700 and 1150 nm, which makes NIR labels of special importance.[20] Near-infrared emitting nanocrystals could in principle be applied to in vivo biomedical application (imaging and labeling) where detection may occur through 1−20 mm of tissues.[20−22]

In contrast to the cadmium chalcogenide nanocrystals, production of lead chalcogenide semiconductor nanocrystals (PbS, PbSe, and PbTe) has only recently been explored.[23−27] Lead chalcogenide semiconductor nanocrystals were first generated inside polymer and oxide glass hosts over a decade ago.[28,29] A more versatile liquid-phase synthesis for PbSe colloidal nanocrystals was first reported by Murray et al. in 2001.[25] In the

* Corresponding author. E-mail: colvin@rice.edu.

(1) Alivisatos, A. P. *J. Phys. Chem. B* **1996**, *100*, 13226−13239.
(2) Alivisatos, A. P. *Science* **1996**, *271*, 933.
(3) Review articles on colloidal nanocrystals. *Acc. Chem. Res.* **1999**, *32*, 387 (Special Issue for Nanostructures).
(4) Peng, X.; Wickham, J.; Alivisatos, A. P. *J. Am. Chem. Soc.* **1998**, *120*, 5343−5344.
(5) Murray, C. B.; Norris, D. J.; Bawendi, M. G. *J. Am. Chem. Soc.* **1993**, *115*, 8706−8715.
(6) Peng, X.; Manna, L.; Yang, W. D.; J.Wickham; Scher, E.; Kadavanich, A.; Alivisatos, A. P. *Nature* **2000**, *404*, 59.
(7) Quantum Dot Corporation, http://www.qdots.com.
(8) Chan, W. C. W.; Nie, S. *Science* **1998**, *281*, 2016−2018.
(9) Bruchez, M. Jr.; Moronne, M.; Gin, P.; Weiss, S.; Alivisatos, A. P. *Science* **1998**, *281*, 2013−2016.
(10) Mattoussi, H. M., J. M.; Goodman, E.; Anderson, G. P.; Sundar V. C.; Mikulec, F. V.; Bawendi, M. G. *J. Am. Chem. Soc.* **2000**, *122*, 12142.
(11) Coe, S.; Woo, W.-K.; Bawendi, M. G.; Bulovic, V. *Nature* **2002**, *420*, 800.
(12) Colvin, V. L.; Schlamp, M. C.; Alivisatos, A. P. *Nature* **1994**, *370*, 354.
(13) Tessler, N.; Medvedev, V.; Kazes, M.; Kan, S.; Banin, U. *Science* **2002**, *295*, 1506.
(14) Klimov, V. I.; Mikhailovsky, A. A.; Xu, S. M., A.; Hollingsworth, J. A.; Leatherdale, C. A.; Eilser, H.-J.; Bawendi, M. G. *Science* **2000**, *290*, 314.
(15) Kazes, M.; Lewis, D. Y.; Ebenstein, Y.; Mokari, T.; Banin, U. *Adv. Mater.* **2002**, *14*, 317.
(16) Huynh, W. U. D., J. J.; Alivisatos, A. P. *Nature* **2002**, *295*, 2425.
(17) Eisler, H.-J.; Sundar, V. C.; Bawendi, M. G.; Walsh, M.; Smith, H. I.; Klimov, V. I. *Appl. Phys. Lett.* **2002**, *80*, 4614.
(18) Wise, F. W. *Acc. Chem. Res.* **2000**, *33*, 773−780.
(19) Yu, W. W.; Qu, L.; Guo, W.; Peng, X. *Chem. Mater.* **2003**, *15*, 2854−2860.
(20) Lim, Y. T.; Kim, S.; Nakayama, A.; Stott, N. E.; Bawendi, M. G.; Frangioni, J. V. *Mol. Imaging* **2003**, *2*, 50−64.
(21) Richards-Kortum, R.; Drezek, R.; Sokolov, K.; Pavlova, I.; Follen, M. In *Handbook of Biomedical Fluorescence*; Mycek, M.-A., Pogue, B. W., Eds.; Marcel Dekker, Inc.: New York, 2003, pp 237−264.
(22) Weissleder, R. *Nat. Biotechnol.* **2001**, *19*, 316−317.
(23) Sashchiuk, A.; Langol, L.; Chaim, R.; Lifshitz, E. *J. Cryst. Growth* **2002**, *240*, 431−438.
(24) Lifshitz, E.; Bashouti, M.; Kloper, V.; Kigel, A.; Eisen, M. S.; Berger, S. *Nano Lett.* **2003**, *3*, 857−862.
(25) Murray, C. B.; Sun, S.; Gaschler, W.; Doyle, H.; Betley, T. A.; Kagan, C. R. *IBM J. Res. Dev.* **2001**, *45*, 47−55.
(26) Wehrenberg, B. L.; Wang, C.; Guyot-Sionnest, P. *J. Phys. Chem. B* **2002**, *106*, 10634−10640.
(27) Du, H.; Chen, C.; Krishnan, R.; Krauss, T. D.; Harbold, J. M.; Wise, F. W.; Thomas, G.; Silcox, J. *Nano Lett.* **2002**, *2*, 1321−1324.

10.1021/cm049476y CCC: $27.50
Published on Web 07/17/2004

following year, Guyot-Sionnest,[26] Krauss,[27] and their coworkers simultaneously reported similar methods to prepare PbSe semiconductor colloidal nanocrystals. Very small PbSe nanocrystals ($d = 2-3$ nm)[23] as well as larger PbSe quantum wires, rods, and cubes[24] have also been recently reported.

Here, we report our study which uses a noncoordinating solvent to synthesize PbSe nanocrystals. Analogous to nanocrystalline CdSe, a noncoordinating solvent permits the formation of a larger size range of PbSe nanoparticles in a cheap and environmentally friendly solvent.[19,30,31] Moreover, the reaction yields materials equivalent in quality to current cadmium chalcogenide materials. Typical size distributions are between 5 and 7% prior to any size-selective treatments. The near-infrared absorption of these materials ranges from 1100 to 2520 nm (corresponding to diameters of 3−13 nm) and a strong (QY > 85%) NIR emission is observed. Finally, we demonstrate a simple method for transferring the as-made organically soluble materials into water.

Experimental Section

Materials. Lead oxide (99.999%), oleic acid (90%), selenium (99.5%, 100 mesh), trioctylphosphine (90%), 1-octadecene (90%), tetrachloroethylene (99%), and 11-mercaptoundecanoic acid (95%) were purchased from Aldrich. Chloroform, methanol, hexane, toluene, and acetone were obtained from Fisher.

Synthesis. PbSe semiconductor nanocrystals were synthesized in a three-neck flask equipped with condenser, magnetic stirrer, thermocouple, and heating mantle. Typically, a mixture of 0.892 g of PbO (4.00 mmol), 2.825 g of oleic acid (10.00 mmol), and technological grade 1-octadecene (ODE) (the total weight was 16 g) turned colorless upon heating to around 150 °C; the mixture was further heated to 180 °C. Then, 6.4 g of selenium-trioctylphosphine solution (containing 0.64 g of selenium, 8.00 mmol) was quickly injected into this hot solution; the temperature of the reaction mixture was allowed to cool to 150 °C for the growth of the PbSe semiconductor nanocrystals. All steps in the reactions were carried out under argon. The nanocrystal growth process here is continuous. In a typical reaction, monodisperse 3.5-nm particles were recovered after only 10 s at 150 °C; the yields for these smaller particles were low as much of the starting material remained unreacted. Longer time treatments, of for example 800 s, provided nearly 100% yields of 9.0-nm nanocrystals.

Characterization. A Varian Cary 5000 UV−Vis−NIR spectrophotometer was used to monitor the reaction; aliquots of the solution were removed at different time intervals with a syringe. A Jobin Yvon Spex Fluorolog 3-211 Fluorescence spectrophotometer was used to obtain photoluminescence spectra. X-ray diffraction patterns were recorded by powder diffraction using a Siemens Platform-Model General Area Detector Diffraction System (GADDS) with a Cu Kα source. The powder samples were run with an internal silicon powder standard in order to account for instrumental line broadening. TEM specimens were made by evaporating one to two drops of reaction solution onto carbon-coated copper grids. The TEM micrographs were taken by a JEOL FasTEM 2010 transmission electron microscope operating at 100 kV. The size and size distribution data were obtained by measuring about 10000−15000 individual PbSe nanocrystalline particles using Image-Pro Plus 5.0 (Media Cybernetics Inc.). The microscope was carefully calibrated by standard samples to avoid any systematic error due to incorrect magnification adjustments.

Purification. It should be pointed out that ODE and oleic acid, which show strong absorption in NIR, must be removed from the original aliquots taken from the reaction flask before the absorption measurement. The aliquot was swiftly taken out and quenched by room-temperature chloroform. The chloroform solution was extracted twice with an equal volume of methanol; then the ODE phase was mixed with excess acetone to totally precipitate PbSe semiconductor nanocrystals. The precipitated PbSe semiconductor nanocrystals were redispersed in chloroform or hexane and were precipitated again by excess acetone. The purified PbSe semiconductor nanocrystals (solid state) were finally dispersed in tetrachloroethylene for NIR absorbance and other characterizations. During the purification process, the PbSe semiconductor nanocrystals were completely recovered, and there was no size selection applied to the sample.

Results and Discussion

The advantages of using a noncoordinating solvent in producing semiconductor nanocrystals have been illustrated for a wide range of materials.[19,30−34] This method not only eliminates the extremely toxic organometallic precursors and most phosphine-containing solvents used in other methods but also dramatically decreases the cost of high-quality semiconductor nanocrystals. On the basis of the success of noncoordinating solvents in producing other high-quality nanocrystals, we adopted many of these existing methods when producing PbSe. Lead oxide was used as a lead source, and at 150 °C this material forms lead oleate with oleic acid; the injection of selenium (trioctylphosphine as solvent) at 180 °C starts the nucleation of PbSe. With lowering of the reaction temperature immediately after injection, no further nucleation occurs in the reaction. The temperature remains high enough to permit the nuclei to grow until soluble lead is consumed.

A transmission electron micrograph of the sample (Figure 1) reveals that the nanocrystals develop as highly monodisperse materials without the need for size selection. The as-synthesized PbSe semiconductor nanocrystals are generally spherical dots; the size distribution is very narrow, typically 5−7% except when diameters exceed 10 nm (>10 nm, 10−15% standard deviation). High-resolution TEM micrographs of the PbSe nanocrystals (Figure 2) show that these nanocrystals are single crystals without detectable stacking faults or crystal defects. In contrast to existing reports of larger PbSe crystals, we always find spherical dots even up to the largest sizes (13 nm).[24] Electron diffraction (Figure 3) and X-ray diffraction patterns (Figure 4) of the sample confirm that the nanocrystals are a perfect rock-salt crystal structure. The size calculated from line broadening by the Scherrer equation is 5.7 nm, which is very close to the measured diameter from TEM observation of the same sample (5.9 nm). Table 1 and Table 2 give the observed reflections from electron and X-ray diffraction. The calculated values of *d* spacing, diffraction angle, and intensity are in excellent agreement with the cubic (rock salt) structure of bulk PbSe.[35]

As in all quantum dot systems, PbSe nanocrystals exhibit a blue shift in absorption with decreasing size.

(28) Bakueva, L.; Musikhin, S.; Hines, M. A.; Chang, T.-W. F.; Tzolov, M.; Scholes, G. D.; Sargent, E. H. *Appl. Phys. Lett.* **2003**, *82*, 2895−2897.

(29) Lipovskii, A.; Kolobkova, E.; Petrikov, V.; Kang, I.; Olkhovets, A.; Krauss, T.; Thomas, M.; Silcox, J.; Wise, F.; Shen, Q.; Kycia, S. *Appl. Phys. Lett.* **1997**, *71*, 3406−3408.

(30) Yu, W. W.; Peng, X. *Angew. Chem., Int. Ed.* **2002**, *41*, 2368.

(31) Yu, W. W.; Wang, Y. A.; Peng, X. *Chem. Mater.* **2003**, *15*, 4300−4308.

(32) Battaglia, D.; Peng, X. *Nano Lett.* **2002**, *2*, 1027−1030.

(33) Li, J. J.; Wang, Y. A.; Guo, W.; Keay, J. C.; Mishima, T. D.; Johnson, M. B.; Peng, X. *J. Am. Chem. Soc.* **2003**, *125*, 12567−12575.

(34) Battaglia, D.; Li, J. J.; Wang, Y.; Peng, X. *Angew. Chem., Int. Ed.* **2003**, *42*, 5035−5039.

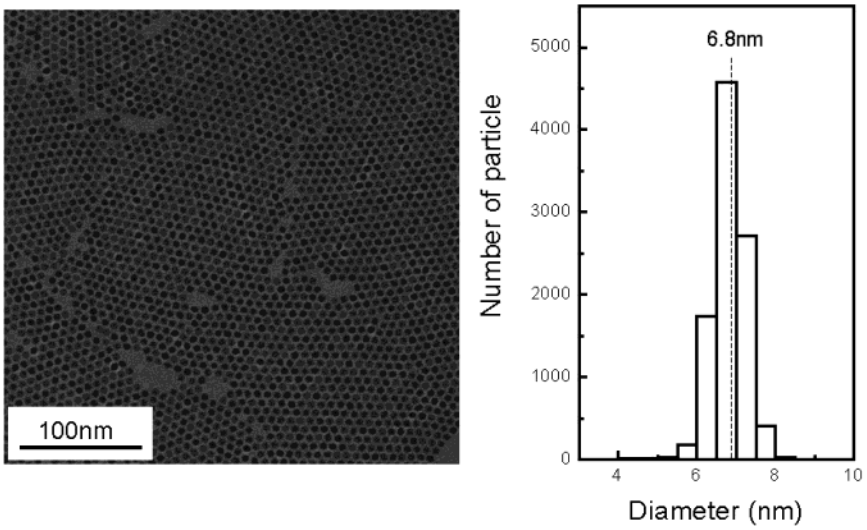

Figure 1. TEM photograph (left) and histogram (right) of the as-prepared PbSe semiconductor nanocrystals. The PbSe semiconductor nanocrystal sample shown here has an average diameter of 6.8 nm with a very narrow size distribution (σ = 6.2%).

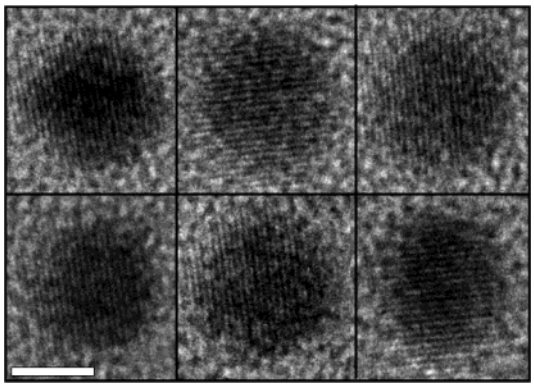

Figure 2. High-resolution TEM photographs of individual PbSe semiconductor nanocrystals. The single-crystal structure is clearly apparent. The white bar in the left-bottom corner is 5 nm.

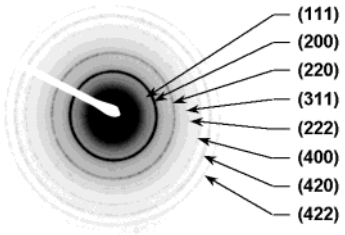

Figure 3. Electron diffractogram of the PbSe nanocrystals. These rings index well to rock-salt PbSe (Table 1).

Figure 5 illustrates the size-dependent spectra of various-sized PbSe semiconductor nanocrystals. Well-defined peaks, which reflect the narrow size distribution, are readily apparent. The first absorption peak ranges from 1100 to 2520 nm, which is the widest available range to date; the HWHM (half width at half maximum to the long wavelength side of the first absorption peak position)[19] is 55−65 nm except for very large sizes (9−13 nm). The HWHM in the existing preparations for PbSe are above 70 nm, except Murray's

(35) McClune, W. F. *Powder Diffraction File Alphabetical Index Inorganic Phase*; JCPDS: Swarthmore, PA, 1980.

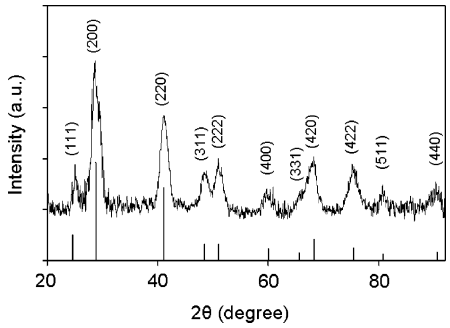

Figure 4. X-ray diffraction pattern of 5.9-nm PbSe nanocrystals indexed to the bulk rock-salt crystal structure. The sample's crystal size as calculated from line broadening by the Scherrer equation is 5.7 nm.

Table 1. Interplanar Spacings Obtained by the Electron Diffractogram of the PbSe Nanocrystals

radius of diffraction circle (mm)	calculated value of *d* (Å)	*d* of PbSe phase from ref 35	*hkl*
6.28	3.5	3.54	111
7.23	3.0	3.06	200
10.26	2.1	2.165	220
12.11	1.8	1.846	311
12.80	1.7	1.768	222
14.54	1.5	1.531	400
16.25	1.4	1.369	420
17.75	1.2	1.250	422

55−60 nm in the narrow peak position range of 1600−1750 nm.[25] It should be noted that our results are based on total recovery of the entire sample.

The size distribution of PbSe nanocrystals changes as the reaction proceeds. It can be seen from Figure 6 that the size distribution is broad at the beginning of the reaction (HWHM is used here as a convenient index of size distribution), but quickly narrows to a stable value of 55 nm. This is a "focusing" of the size distribution similar to that reported by Peng et al.[4] After several minutes the particle size distribution increases due to the depletion of the monomers in the reaction solution; this is the result of defocusing of the size distribution (Ostwald ripening). Monodisperse particles are formed in this reaction because the nucleation process is limited

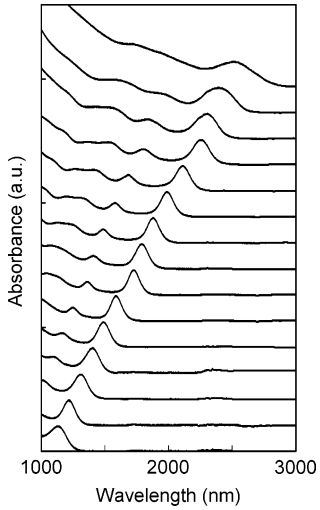

Figure 5. Near-infrared absorption spectra of as-prepared PbSe semiconductor nanocrystals. Four to five features (states) are distinctly resolved.

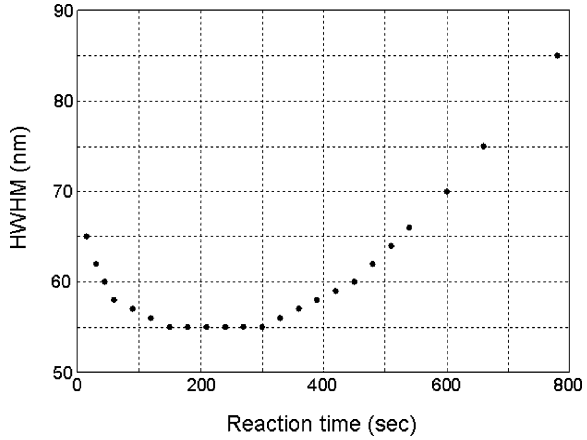

Figure 6. Size distribution variation over the course of the reaction. The reaction started with 4.00 mmol of PbO, 8.50 mmol of oleic acid, 12.283 g of ODE, and 8.00 mmol of Se (with 5.76 g of trioctylphosphine) at 180 °C; the final growth temperature was 150 °C.

Table 2. Comparison of X-ray Diffraction Experimental Results with Bulk Structure of PbSe

literature result from ref 35				this work	
d value (Å)	*hkl*	2*θ* (deg)	intensity (%)	2*θ* (deg)	intensity (%)
3.54	111	25.1	30	25.2	20.5
3.06	200	29.2	100	28.8	100
2.165	220	41.7	70	41.2	62.1
1.84	311	49.5	18	48.5	23.5
1.768	222	51.7	20	51.0	27.3
1.531	400	60.4	14	59.9	11.4
1.405	331	66.5	6	65.7	9.9
1.369	420	68.5	25	68.0	31.1
1.25	422	76.1	16	75.6	25.8
1.179	511	81.6	4	80.8	9.2
1.082	540	90.8	6	90.1	11.4

to the brief injection period; the lower temperature growth occurs slowly and relies predominantly on lead monomers provided at the start of the reaction rather than the dissolution of smaller particles.

We also evaluated the relationship of the first absorption peak (Figure 5) to the nanocrystal size and compared it to other published data (Figure 7). In developing this relationship, both the methods used to size and stabilize particles received great attention so as to minimize error. First, all samples were immediately purified after they were taken out from the reaction flask, and the measurement of the absorption spectra and the TEM sample preparation were quickly completed. This prevented etching and/or oxidation of particles in air. Additionally, the size and size distribution data were obtained by using Image-Pro Plus 5.0 software to count 10000−15000 individual PbSe nanocrystalline particles. The individual particles were measured from 4 to 6 TEM micrographs from different areas on one grid specimen; this greatly reduced the possible error generated from nonuniform drying of particles. As the software requires a number of judgments in the data processing regarding the thresholding and filtering of images, the data reported in Figure 7 show the results for the independent analysis by two individuals. There is good agreement between the two data sets. Finally, to ensure this sizing curve is accurate, multiple samples with the same first absorption peak wavelength were compared. There is little difference (1.7% maximum) in size between different reaction batches.

The data shown in Figure 7 were collected from five different sources including our own.[23,25−27] Kang and Wise[36] performed a four-band envelope function calculation of the electronic structures of PbSe nanocrystals. The theoretical results were also plotted in Figure 7 (symbol with ×), which offset our data by 1.5−2.5 nm. In contrast to the well-studied CdSe semiconductor nanocrystal materials, the size versus absorption peak data from different studies are not in perfect agreement. While there is reasonable agreement from 1000 to 1400 nm (first absorption peak position), more substantial variations are observed beyond 1500 nm. Such differences may be due to experimental factors associated with particle stabilization or sizing. Alternatively, we note that PbSe is a material which exhibits much stronger quantum confinement than CdSe, due to the large exciton diameter in the bulk material. In this case, the relationship between particle diameter and optical absorption properties would not be universal for all reaction strategies; however, the differences should be more pronounced at smaller sizes in contrast to our data which show greater differences at larger sizes. Alternatively, subtle changes in crystal habit or shape at larger sizes in different preparations could lead to variations in the optical absorption spectrum.

The as-synthesized PbSe semiconductor nanocrystals have a strong near-infrared emission. Figure 8 shows the absorption and emission spectra of one sample. The first absorption peak position is 1205 nm (HWHM is 56 nm); the emission (PL, photoluminescence) peak position is 1235 nm (fwhm (full width at half maximum of the emission spectrum peak) of PL is 145 nm). There is a 30-nm Stokes shift. The PL spectrum is also a perfect Gaussian shape and clearly indicates a pure band-gap emission. The quantum efficiency was measured as 89% for this sample using IR-26 as a reference,[26] which is similar to reported results for PbSe.[26,27] This result is typical for the smaller lead selenide particles (d < 4.5 nm); similar experiments on larger near-infrared quantum dots are underway.

(36) Kang, I.; Wise, F. W. *J. Opt. Soc. Am. B* **1997**, *14*, 1632−1646.

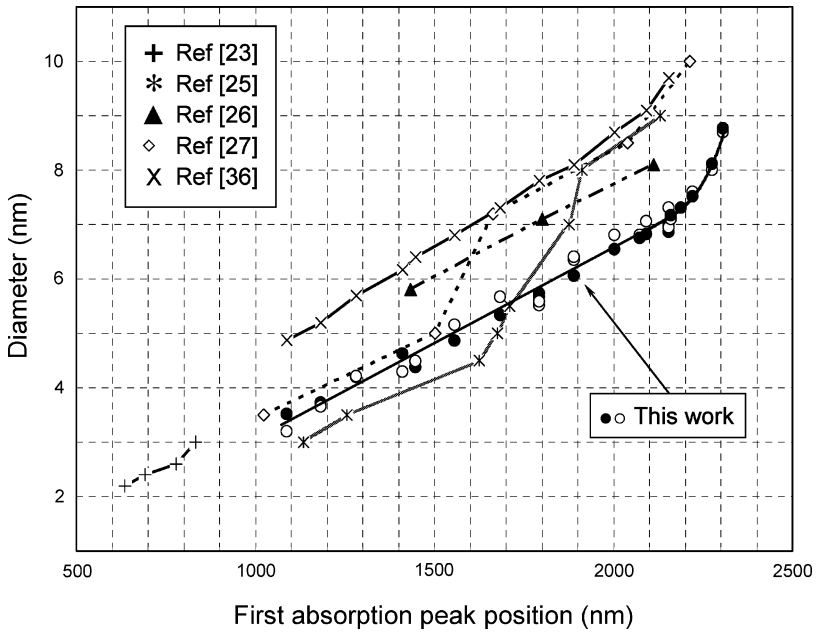

Figure 7. Diameter of semiconductor nanocrystals versus the position of the first absorption peak. Data were taken from this work as well as other recently published reports. The open and solid circles are from two individuals' independent measurements and demonstrate that little systematic error is introduced in the sizing process.

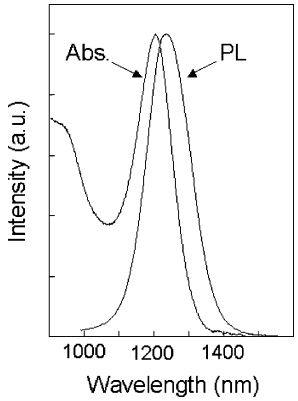

Figure 8. Absorption and emission (PL) spectra of 3.9-nm PbSe semiconductor nanocrystals. The narrow near-infrared emission is pure band-gap emission with a quantum efficiency of 89%.

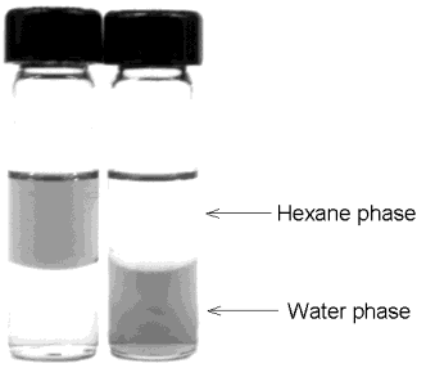

Figure 9. Water-soluble PbSe semiconductor nanocrystals. Initially, the materials are soluble in organic solvents, as shown on the left where the organic phase has a distinctive brown-black color due to the presence of PbSe nanocrystals. The material can be derivatized for water solubility as is shown on the right, where the colored nanocrystals are now in the aqueous phase.

The as-prepared PbSe are oleate-stabilized nanocrystals and are soluble in organic solvents such as toluene, chloroform, and hexane. However, for biological imaging applications water-soluble materials are essential. It is straightforward to make water-soluble PbSe semiconductor nanocrystals through exchange of hydrophobic ligands for hydrophilic ligands. Here, water-soluble PbSe semiconductor nanocrystals were successfully obtained by using 11-mercaptoundecanoic acid as the new capping ligand following a method developed for CdSe.[37] Figure 9 shows clearly the transfer of the black PbSe nanocrystal material from the oil phase to the water phase after this exchange process. The absorption and photoluminescence spectra of these nanoscale PbSe's in water are unchanged from that of the original materials; however, the quantum yield of emission falls somewhat in water, to 35% from 89%. While these materials are stable in pure water, in some biological buffers the materials do not remain in solution. Optimization of these surface-capping strategies, and a more detailed study on the application of these water-soluble NIR emitters to in vivo biological applications, is underway.

Conclusion

Monodisperse PbSe semiconductor nanocrystals with a rock-salt structure were successfully synthesized in a noncoordinating solvent. The high quality, wide optical absorption range, and high quantum efficiency of the as-prepared PbSe semiconductor nanocrystals illustrate the value of using noncoordinating solvents in chalcogenide syntheses.

Acknowledgment. We would like to thank Dr. Sergei M. Bachilo and Dr. R. Bruce Weisman for the use of the Jobin Yvon Spex Fluorolog 3-211 Fluorescence spectrophotometer. This work was financially supported by the National Science Foundation through the Center for Biological and Enviromental Nanotechnology [EEC-0118007], and the Robert A. Welch Foundation [C-1349].

CM049476Y

(37) Aldana, J.; Wang, Y. A.; Peng, X. *J. Am. Chem. Soc.* **2001**, *123*, 8844−8850.